WORLD JOURNAL OF PHARMACEUTICAL RESEARCH
Coden USA: WJPRAP Impact Factor 8.453
Volume 15, Issue 1, 1061-1087. Research Article ISSN 2277–7105

FORMULATION AND EVALUATION OF DIFUNISAL-LOADED NANOSTRUCTURED LIPID CARRIER-BASED GEL FOR ENHANCED TOPICAL DRUG DELIVERY

Shivani Rathor[1]*, Dr. Tanu Bhargava[2], Dr. Praveen Khirwadkar[3]

Institute of Pharmacy Samrat Vikramaditya Vishwavidyalaya, Ujjain.

Article Received on 04 Dec. 2025,
Article Revised on 23 Dec. 2025,
Article Published on 01 Jan. 2026,

https://doi.org/10.5281/zenodo.18095387

***Corresponding Author**

Shivani Rathor

Institute of Pharmacy Samrat Vikramaditya Vishwavidyalaya, Ujjain.

How to cite this Article: Shivani Rathor[1]*, Dr. Tanu Bhargava[2], Dr. Praveen Khirwadkar[3]. (2026). FORMULATION AND EVALUATION OF DIFUNISAL-LOADED NANOSTRUCTURED LIPID CARRIER-BASED GEL FOR ENHANCED TOPICAL DRUG DELIVERY. World Journal of Pharmaceutical Research, 15(1), 1061–1087.

ABSTRACT

The present study focuses on the development and evaluation of a nanostructured lipid carrier (NLC)-based gel formulation for the topical delivery of Diflunisal, a poorly water-soluble non-steroidal anti-inflammatory drug (NSAID). The objective was to enhance dermal penetration, achieve sustained drug release, and minimize systemic side effects associated with oral administration. NLCs were prepared using cold pressure homogenization followed by ultrasonication, employing a combination of solid and liquid lipids along with a suitable surfactant. The formulation was characterized for particle size, polydispersity index, zeta potential, entrapment efficiency, and in vitro drug release. FTIR spectroscopy confirmed the absence of significant drug-excipient interactions, indicating chemical compatibility. UV spectrophotometric analysis was performed at 258 nm to confirm drug identity and support quantitative analysis. The optimized NLCs were incorporated into a carbopol-based gel and evaluated for physicochemical properties including pH, viscosity, spreadability, and drug content. In vitro diffusion studies demonstrated a sustained release profile of Diflunisal from the NLC gel compared to conventional formulations. These findings suggest that the developed Diflunisal-loaded NLC gel is a promising strategy for improved topical drug delivery, offering enhanced skin penetration, prolonged release, and better therapeutic potential.

INTRODUCTION

A novel kind of nanoscale medication delivery is called nano-structural lipid carriers (NLCs). technology, which could improve the stability, solubility, and bioavailability of a number of drugs and bioactive substances. NLCs consist of a liquid lipid layer encircling a solid lipid core, creating a heterogeneous matrix that can hold a wide range of chemicals. In several aspects, such as biocompatibility, scalability, adaptability, and cost-effectiveness, NLCs outperform alternative nanocarriers such liposomes, solid lipid nanoparticles, and polymeric nanoparticles. I'll go over the current state of the art for NLCs, including characterization methods, preparation procedures, and applications in a range of biotechnology and medical domains, as well as the difficulties and prospects for more research and development.[1] Diflunisal is primarily used to treat rheumatoid arthritis, osteoarthritis, and primary dysmenorrhea. Additionally, the anticancer effects of diflunisal were shown.[2] The therapeutic use of diflunisal in the treatment of cardiac amyloidosis, as demonstrated by clinical research, has garnered attention in recent years.[3-8]

A possible treatment for transthyretin (TTR) polyneuropathy, a disorder that damages nerves, is diflunisal. Its efficacy and safety are being evaluated through human clinical trials and animal safety investigations. By attaching itself to TTR, diflunisal stops it from misfolding and aggregating, which can harm nerves.

Its efficacy and safety are being evaluated through human clinical trials and animal safety investigations. By attaching itself to TTR, diflunisal stops it from misfolding and aggregating, which can harm nerves. The goal of this research is to offer a less harmful substitute for existing therapies.[9] The nonrandomized study demonstrated that diflunisal has a survival benefit similar to that of clinically approved tafamidis.[10]

These results make diflunisal a promising medication to treat cardiac amyloidosis, as the first approved medication for the treatment of Transthyretin Amyloid Cardiomyopathy (ATTR-CM) was only proposed in 2019.[11] Non-steroidal anti-inflammatory drug (NSAID) use for an extended period of time can result in a number of dangerous side effects.

These include fluid retention, hypertension, gastrointestinal (GI) bleeding and ulceration (associated with COX-1 inhibition), and renal impairment (associated with COX-2 inhibition). Due to prolonged COX-2 suppression, these problems may cause individuals to develop heart failure.[12-14] Because diflunisal is hydrophobic—that is, it repels water—it does

not mix well with water. This makes it difficult for the body to efficiently absorb and distribute the medication, which results in less-than-ideal outcomes for the body's processing and utilization of it.[15]

The complexity of diflunisal is increased by its photosensitivity and photoproduct toxicity.

Due to the drug's importance and acknowledged limitations, new delivery methods for diflunisal must be developed in order to reduce side effects, improve stability, and improve pharmacokinetic profile and biodistribution. This study includes all available information on the incorporation of diflunisal into various drug delivery systems.

MATERIALS AND METHODS

Fourier transform infrared (FTIR) and melting point spectroscopy have been used in the preformulation research to find Difunisal. The drug samples' physical characteristics, color, and odor were assessed.

Solubility

It is a white, solid powder that is soluble. Because of its solubility, it can be used in a variety of solvents. Slightly soluble in phosphate buffer and soluble in methanol and DMSO. The low water solubility of diflunisal may affect its absorption and bioavailability. This involved precisely weighing 50 mg of diflunisal medication and testing its solubility in 50 ml of pure water, phosphate buffer (7.4 pH), methanol, acetone, and toluene. The medication was discovered to be nearly insoluble in toluene and acetone, slightly soluble in phosphate buffer, and easily soluble in methanol and ethanol. Methanol was used as the diluent because these materials are easily accessible, and stability studies revealed that the medication remained stable in methanol. Additionally, difunisal dissolves in a solution of sodium salicylate.[16]

Melting point

First, move the drug sample for diflunisal from one end of a thick-walled capillary tube. Gently tap the tube to ensure that the sample is packed at the bottom.

It is necessary to insert the filled capillary tube into the digital melting point apparatus. Heating Procedure: Gradually and steadily increase the device's temperature (usually 1-2°C per minute). Examine the sample by using a magnifying glass. Note the temperature at which the sample starts to melt (beginning of melting) and when it completely melts (clear liquid).

Spectroscopic Analysis

Determination of absorption maxima (λ max)

Standard Stock Solution Preparation

A 10 mL volumetric flask was filled with precisely weighed 10 milligrams of diflunisal. To guarantee full drug solubilization, 4 mL of sodium salicylate solution was added, and the flask was shaken for a minute. A standard stock solution with a concentration of 1 mg/mL was then created by adding distilled water to the capacity. Additional working standard solutions were prepared using this stock solution.[17]

Preparation of Standard Graph

To create standard solutions with concentrations of 2, 4, 6, and 8 µg/mL, appropriate aliquots were taken from the previously prepared standard stock solution and diluted with distilled water. Using distilled water as a blank, the absorbance of each solution was measured at 258 nm using a UV–Visible spectrophotometer. Plotting absorbance against concentration allowed for the creation of a standard graph.

Preparation of Calibration Curve

Standard solutions with concentrations between 2 and 8 µg/mL were used to create the Diflunisal calibration curve. Each solution's absorbance was measured at 258 nm using pure water as a blank. Plotting the calibration curve involved putting absorbance on the y-axis and concentration on the x-axis. Diflunisal was quantitatively estimated in the formulation using the calibration curve.

Drug- excipient Compatibility Studies

Method 1: a small quantity of the medication, that is, the drug's body mixture along with the auxiliary chemicals (in a ratio of 1:1 was prepared for a potential interaction) was put in an excess bottle and sealed with a rubber cap. The sample was stored for two weeks at 60 °C then for two months at 40 °C.

The sample was physically examined for liquefaction, caking, gas or odor production, and variations following storage. FTIR spectroscopy was used in Method 2 to examine the apparent drug and auxiliary agent mixture.

Formulation of Difunisal loaded of Nanostructured Lipid Carriers (NLCs) gel[18]

Preparation of NLCs18via Melt Emulsification and Cold Solidification

NLCs were formulated using the melt emulsification followed by low-temperature solidification technique. Glyceryl monostearate (GMS) and oleic acid were melted together at 80 °C to form the lipid phase. Simultaneously, the aqueous phase was prepared by dissolving Poloxamer 407 and Tween 80 in 10 mL of distilled water and heating it to the same temperature to ensure uniformity.

Diflunisal, dissolved in 0.5 mL DMSO, was incorporated into the molten lipid phase under constant stirring. This drug-lipid mixture was then gradually introduced into the hot aqueous phase while maintaining stirring at 80 °C to produce a coarse emulsion.

The emulsion was rapidly cooled in an ice bath and homogenized at varying speeds, followed by probe sonication (Orchid Scientific and Innovative India Pvt. Ltd.) for 10 minutes to achieve nanoscale dispersion. The final NLCs were stored under refrigeration for subsequent analysis.

Table 1: Various of Nanostructured Lipid Carriers Formulations.

Formulation Code	Solid lipid (GMS)	Liquid Lipid (OleicAcid) ML	Poloxamer 407	Tween 80 (ML)	DMSO (ML)	Drug (Mg)	Distilled Water	Homogenisation speed (rpm)
F1	40	0.067	50	0.0236	0.5	50	10	1500
F2	50	0.056	38	0.0358	0.5	50	10	2100
F3	70	0.0335	50	0.0236	0.5	50	10	2500
F4	30	0.0782	25	0.0472	0.5	50	10	2300
F5	50	0.056	50	0.0236	0.5	50	10	2500

Preparation of gel formulation

Preparation of NLC-Based Gel[19]

Drug-loaded NLC batches with high entrapment efficiency were selected for gel formulation. Carbopol was dispersed in purified water and allowed to swell fully. The NLC dispersion was gradually blended into the hydrated Carbopol base with gentle stirring. Triethanolamine was added dropwise to neutralize the mixture and achieve the desired gel consistency. Parabens were incorporated as preservatives, and the final gel was left to equilibrate for 24 hours before evaluation.

EVALUATION METHODS

Determination of Drug Entrapment Efficiency (EE%) and Drug Loading Capacity (LC%)[20]

Entrapment Efficiency and Drug Loading Determination

Entrapment efficiency (EE%) and loading capacity (LC%) of the prepared nanostructured lipid carriers (NLCs) were evaluated using an indirect centrifugation method. A known quantity of NLC dispersion was centrifuged at 4000 g for 8 minutes at 4 °C to separate the unentrapped drug. The supernatant was collected and analyzed using UV–visible spectrophotometry at the drug's maximum absorbance wavelength (λmax). No interference from lipids or other excipients was observed during analysis.

Formulas

$$\%EE=[(\text{Amount of Drug Entrapped}/\text{Total Amount of Drug used})x\ 100$$

Drug Loss = Initial amount of Drug -Amount of Drug Entrapped / Initial amount of Drug

pH

pH Determination of Diflunisal-Loaded NLC Gel

The pH of the diflunisal-loaded NLC gel was measured using pH indicator paper. Approximately 1 g of gel was dispersed in 10 ml of distilled water and gently stirred to form a uniform solution. A pH strip was immersed in the mixture, and the resulting color change was compared against the standard reference chart provided with the indicator paper.

Viscosity Measurement[21]

The viscosity of the NLC gel was evaluated using a Brookfield viscometer. Approximately 1 g of gel was placed in a beaker, and measurements were taken at 20 rpm for 60 seconds using spindle no. 12 at a controlled temperature of 30 °C.

SpreadabilityTest[22]

Spreadability of the NLC gel was evaluated by placing a fixed amount of gel between two glass slides, followed by applying a known weight on the upper slide. The time (T) required for the slides to separate under the applied force was recorded. A shorter separation time indicates better spreadability. It was calculated using the formula:

$$S = M.L/T$$

Where:

- S = Spreadability (g·cm/s)

- M = Weight applied on the upper slide (g)
- L = Length of the glass slide (cm)
- T = Time taken for slide separation (s)

In Vitro Drug Release Study[23]

The in vitro release of the NLC formulation was assessed using a USP type II (paddle) dissolution apparatus. An amount of NLC dispersion equivalent to 10 mg of drug was added to 900 mL of phosphate buffer (pH 7.4) maintained at 37 ± 0.5 °C, with the paddle rotating at 50 rpm. At specified intervals (0, 15, 30, 60, 120, 240, and 360 minutes), 5 mL samples were withdrawn and replaced with equal volumes of pre-warmed buffer to maintain sink conditions. Samples were filtered through a 0.45 µm membrane and analyzed at 258 nm using a UV–visible spectrophotometer. The cumulative drug release was calculated and plotted over time to determine the release profile.

In vitro drug release Of Optimised NLC Gel

The in-vitro drug release of the optimized NLC gel formulation was evaluated using an egg membrane diffusion method. The egg membrane was mounted over the open end of a glass test tube containing the gel formulation. The assembly was immersed in phosphate buffer saline (PBS, pH 7.4), which served as the receptor medium.

The study was carried out for 10 hours, and samples were withdrawn from the receptor medium at 1-hour intervals. Each withdrawn sample was analyzed for drug content using a UV–visible spectrophotometer, and the cumulative percentage drug release was calculated.

- **Stability Studies**

The physical, chemical, and rheological stability of Diflunisal-Loaded NLC Gel was assessed over one month under various storage conditions to estimate shelf life. Samples were stored at room temperature (25 ± 2 °C), refrigeration (4 ± 2 °C), and accelerated conditions (40 ± 2 °C). At weekly intervals and after one month, the gels were evaluated for changes in appearance, color, phase separation, and spreadability.

RESULT AND DISCUSSION

Preformulation Studies

The organoleptic and physicochemical properties of diflunisal were evaluated prior to formulation development. Diflunisal was observed as a white to off-white crystalline powder

with no characteristic odour. The drug exhibited a high melting point, indicating its crystalline nature and thermal stability. Solubility studies revealed that diflunisal is practically insoluble in distilled water, while it showed good solubility in organic solvents such as methanol and ethanol. These properties confirm the hydrophobic nature of diflunisal, which justifies the need for lipid-based nano-carrier systems to enhance its solubility and release characteristics.

Table 2: Organoleptic and Physicochemical Properties of Diflunisal.

S.no.	Property	Interference
1	Colour	White to off -White
2	State	Crystalline powder
3	Odour	Odourless
4	Taste	Slightly bitter
5	Melting point	207-213 °C
6	Solubility	Practically insoluble in water; soluble in methanol and ethanol

UV spectrometer analysis. – peak pick UV spectrum report of diflunisal.

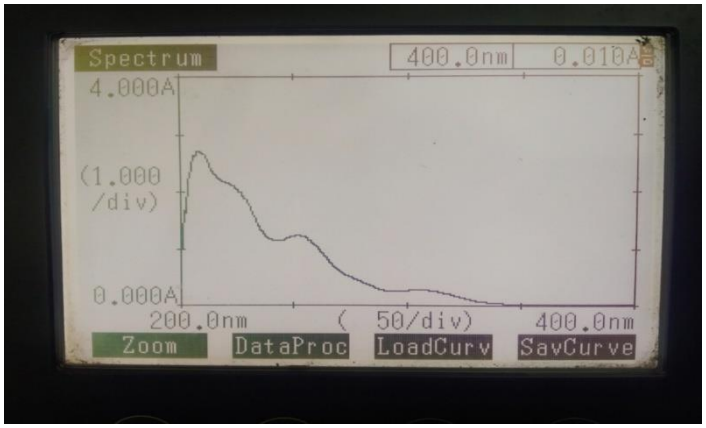

Standard calibration curve

Table 3: Calibration data of difunisal in sodium salicylate solution at 258 nm.

S.no	Concentration in (µg/ml)	Absorbance at 258 nm
0	0	0
1	2(µg/ml)	0.422
2	4(µg/ml)	0.792
3	6(µg/ml)	1.063
4	8(µg/ml)	1.599

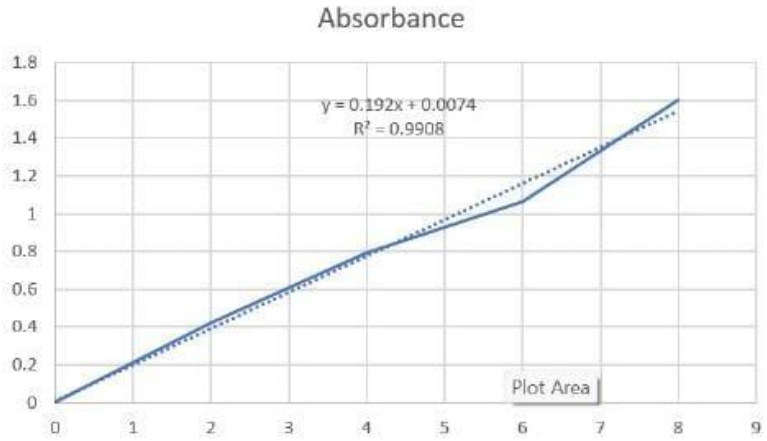

Fig. 1: Standard graph of Difunisal Drug.

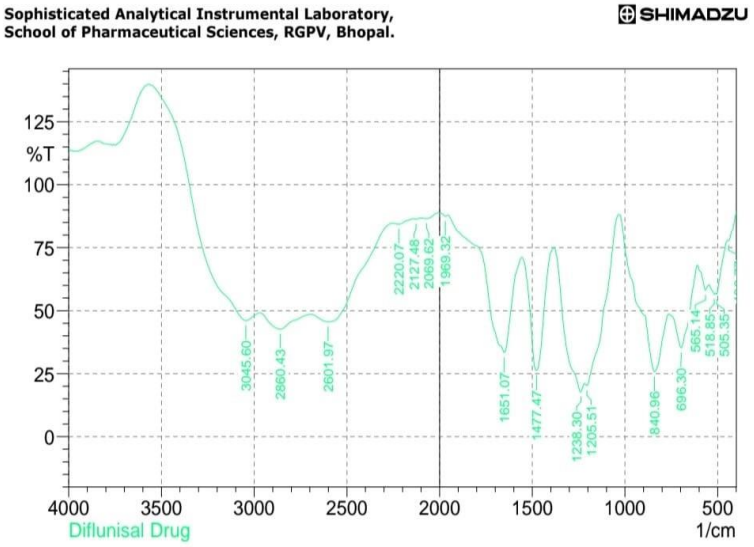

No.	Peak	Intensity	Corr. Intensity	Base (H)	Base (L)	Area	Corr. Area
1	439.77	77.83	1.62	445.56	399.26	3.89	0.35
2	505.35	56.51	1.75	509.21	447.49	10.58	0.17
3	518.85	56.54	1.21	545.85	511.14	8.24	0.16
4	565.14	58.17	4.3	609.51	547.78	12.74	0.74
5	696.3	35.26	21.81	761.88	611.43	50.33	14.32
6	840.96	25.73	34.41	1029.99	763.81	86.78	37.68
7	1205.51	20.28	5	1217.08	1031.92	65.94	2.04
8	1238.3	17.74	9.81	1381.03	1219.01	77.53	12.72
9	1477.47	26.19	46.74	1556.55	1382.96	53.65	30.02
10	1651.07	33.36	41.67	1953.89	1558.48	83.83	43.39
11	1969.32	87.49	0.74	1994.4	1955.82	2.15	0.07
12	2069.62	86.52	0.93	2102.41	2004.04	5.78	0.23
13	2127.48	86.35	0.27	2142.91	2104.34	2.43	0.03
14	2220.07	84.33	0.97	2258.64	2144.84	7.94	0.27
15	2601.97	45.6	10.4	2690.7	2260.57	97.99	15.73
16	2860.43	42.67	6.24	2968.45	2692.63	93.59	7.75
17	3045.6	46.06	14.72	3554.81	2970.38	66.38	24.85

FTIR Spectral Interpretation of Diflunisal

The Fourier-transform infrared (FTIR) spectrum of Diflunisal exhibited distinct absorption bands indicative of its functional moieties:

Hydroxyl and Carboxylic Acid Groups: A broad absorption band spanning **3200–3600 cm^{-1}** corresponds to O–H stretching vibrations, confirming the presence of both phenolic and carboxylic acid functionalities.

Carbonyl Group: A prominent peak in the **1680–1710 cm⁻¹** region is characteristic of **C=O stretching**, affirming the carboxylic acid group.

Aromatic Framework: Absorptions between **1600–1500 cm⁻¹** are attributed to **C=C stretching** within the aromatic ring, supporting the presence of an aryl system.

C–H Stretching

Aromatic C–H: Bands near **3000–3100 cm⁻¹** indicate aromatic C–H stretching.

Aliphatic C–H: Peaks around **2900 cm⁻¹** suggest minor aliphatic C–H contributions.

C–O Stretching: Absorptions in the **1200–1300 cm⁻¹** range are consistent with **C–O stretching** vibrations from phenolic and carboxylic acid groups.

C–F Stretching: Notable bands between **1000–1300 cm⁻¹** are assigned to **C–F stretching**, confirming fluorine substitution on the aromatic ring. These spectral features collectively validate the structural integrity and functional group composition of Diflunisal.

FTIR of Drug + Excipients

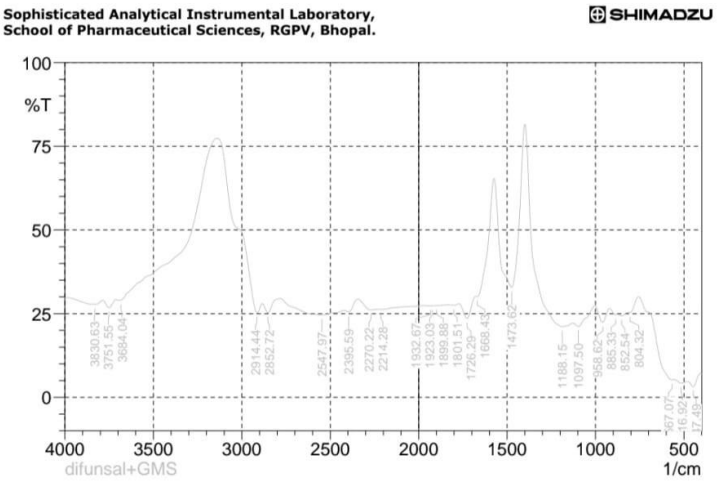

No.	Peak	Intensity	Corr. Intensity	Base (H)	Base (L)	Area	Corr. Area
1	447.49	3.194	2.616	480.28	408.91	96.15	7.989
2	516.92	4.194	0.791	555.5	482.2	98.133	2.677
3	567.07	5.225	1.431	700.16	557.43	137.812	6.032
4	804.32	25.322	0.996	815.89	758.02	32.753	0.51
5	852.54	24.356	0.649	873.75	817.82	33.926	0.338
6	885.33	24.681	0.455	920.05	875.68	26.488	0.219
7	958.62	22.398	4.461	1002.98	921.97	49.427	3.213
8	1097.5	21.189	2.254	1128.36	1004.91	77.849	2.775
9	1188.15	21.089	13.863	1398.39	1130.29	144.213	43.988
10	1473.62	32.82	41.854	1573.91	1400.32	60.388	36.731
11	1668.43	30.072	2.787	1676.14	1575.84	38.885	3.896
12	1726.29	23.515	5.538	1774.51	1678.07	55.793	4.026
13	1801.51	27.513	0.31	1830.45	1776.44	30.163	0.153
14	1899.88	27.39	0.019	1903.74	1832.38	39.976	0.012
15	1923.03	27.314	0.016	1926.89	1903.74	13.032	0.003
16	1932.67	27.313	0.014	1967.39	1928.82	21.717	0.006
17	2214.28	26.247	0.029	2220.07	1969.32	143.026	0.04
18	2270.22	26.079	1.404	2343.51	2222	69.164	1.486
19	2395.59	25.485	1.514	2418.74	2345.44	41.805	0.88
20	2547.97	24.634	2.547	2783.28	2420.66	213.169	10.727
21	2852.72	25.26	3.228	2883.58	2785.21	55.107	1.901
22	2914.44	25.257	8.398	3138.18	2885.51	85.492	4.628
23	3684.04	28.959	0.757	3691.75	3140.11	199.932	22.165
24	3751.55	26.796	2.231	3784.34	3711.04	40.665	1.309
25	3830.63	27.77	0.288	3838.34	3786.27	28.633	0.185

Comment;
difunsal+GMS

Date/Time; 5/13/2025 2:33:45 AM
No. of Scans;
Resolution;

FTIR Analysis of Diflunisal–Glyceryl Monostearate (GMS) Mixture

The FTIR spectrum of the Diflunisal–GMS mixture revealed distinct absorption bands attributable to both components. A broad band between **3200–3600 cm⁻¹** corresponded to **O–H stretching**, indicating the presence of hydroxyl groups from GMS and the carboxylic acid moiety of Diflunisal. Strong absorptions in the **2850–2920 cm⁻¹** range were assigned to **aliphatic C–H stretching** of GMS's long hydrocarbon chains. A sharp band near **1700–1740 cm⁻¹** confirmed **C=O stretching** from both the ester groups of GMS and the carboxylic acid of Diflunisal. Peaks within **1600–1500 cm⁻¹** were attributed to **aromatic C=C stretching**, verifying the intact aromatic structure of Diflunisal. The absence of new or missing characteristic peaks suggested no chemical interaction between the drug and lipid, supporting their **compatibility for NLC formulation**.

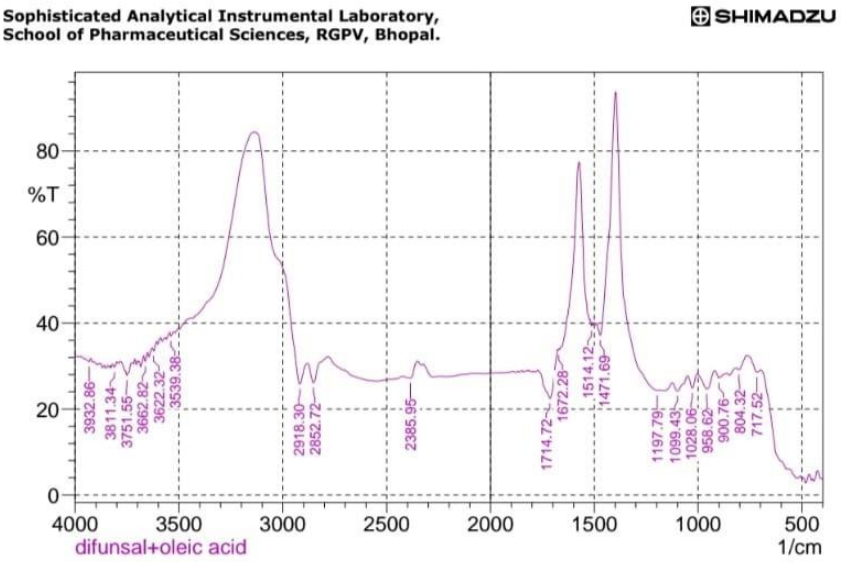

No.	Peak	Intensity	Corr. Intensity	Base (H)	Base (L)	Area	Corr. Area
1	717.52	28.554	1.394	767.67	700.16	34.945	0.333
2	804.32	29.139	0.997	813.96	767.67	23.947	0.365
3	900.76	27.211	1.435	920.05	869.9	27.807	0.52
4	958.62	24.66	3.937	1002.98	920.05	47.819	2.696
5	1028.06	24.864	3.095	1051.2	1002.98	27.797	1.115
6	1099.43	24.197	2.439	1124.5	1051.2	43.495	1.67
7	1197.79	24.315	3.265	1398.39	1188.15	96.237	28.88
8	1471.69	37.155	11.939	1487.12	1398.39	23.821	4.772
9	1514.12	39.316	0.796	1521.84	1510.26	4.606	0.039
10	1672.28	33.702	0.286	1676.14	1668.43	3.631	0.015
11	1714.72	22.466	9.486	1770.65	1676.14	54.843	7.309
12	2385.95	27.156	2.289	2422.59	2353.16	38.231	1.205
13	2852.72	26.111	4.951	2881.65	2781.35	52.944	2.464
14	2918.3	25.835	12.845	3124.68	2881.65	77.803	6.205
15	3539.38	36.956	0.93	3545.16	3523.95	9.037	0.102
16	3622.32	33.485	1.166	3628.1	3608.81	8.958	0.147
17	3662.82	31.086	1.599	3670.54	3651.25	9.542	0.194
18	3751.55	27.831	1.39	3757.33	3728.4	15.566	0.346
19	3811.34	29.705	0.937	3819.06	3799.77	10.023	0.131
20	3932.86	31.017	0.535	3940.57	3925.14	7.79	0.059

Comment;
difunsal+oleic acid

Date/Time; 5/13/2025 2:14:28 AM
No. of Scans;

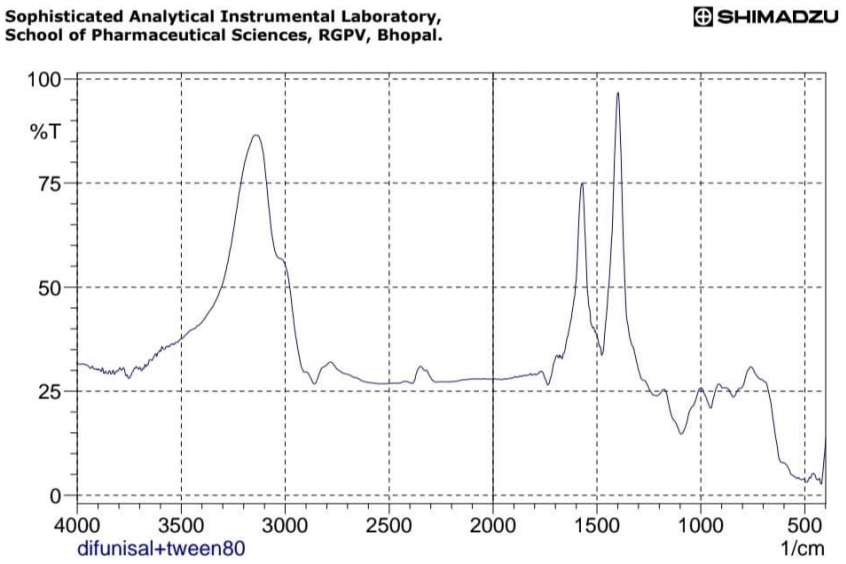

FTIR Analysis of Diflunisal–Tween 80 Mixture

The FTIR spectrum of the Diflunisal–Tween 80 mixture displayed distinct absorption bands attributable to both the drug and the surfactant, indicating their mutual compatibility. A broad band between **3200–3600 cm⁻¹** corresponded to **O–H stretching vibrations** from hydroxyl groups in both Diflunisal and Tween 80. Strong bands in the **2850–2920 cm⁻¹** range were assigned to **aliphatic C–H stretching** of Tween 80's long hydrocarbon chains. The **1700–1720 cm⁻¹** region showed **C=O stretching**, confirming ester functionalities in Tween 80 and the carboxylic acid group of Diflunisal. Peaks between **1600–1500 cm⁻¹** were attributed to **aromatic C=C stretching**, indicating the preserved aromatic structure of Diflunisal. Additionally, bands in the **1100–1300 cm⁻¹** range were linked to **C–O–C stretching** of ester and ether linkages in Tween 80. The retention of all characteristic Diflunisal peaks without significant shifts or loss suggests **no chemical interaction**, affirming the **compatibility of Diflunisal and Tween 80** for formulation purposes.

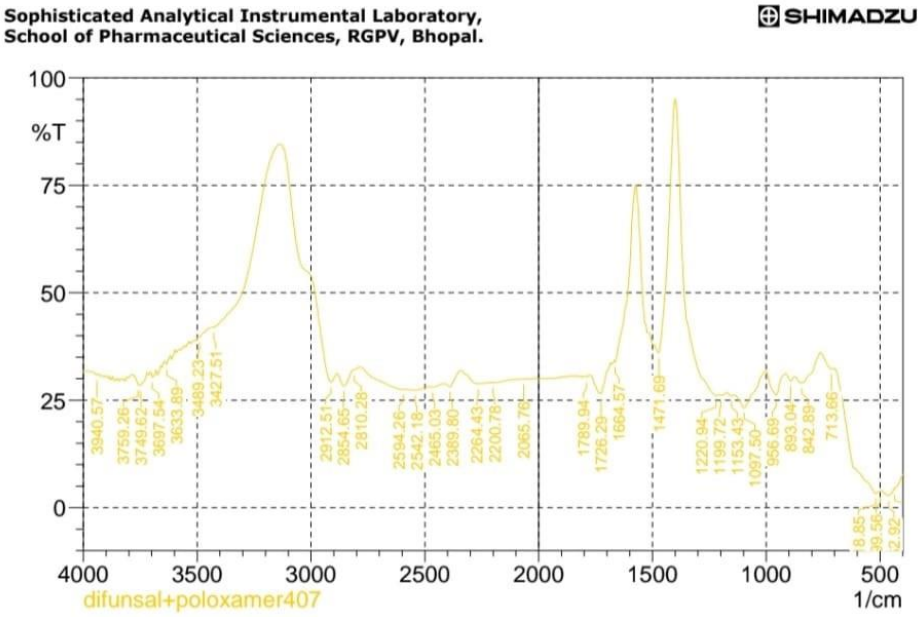

No.	Peak	Intensity	Corr. Intensity	Base (H)	Base (L)	Area	Corr. Area
1	435.91	4.22	0.49	439.77	399.26	50.52	0.9
2	462.92	2.71	1.06	478.35	439.77	57.62	3.11
3	499.56	3.71	0.13	503.42	493.78	13.66	0.06
4	518.85	3.31	0.73	609.51	511.14	122	1.06
5	713.66	32.23	0.8	759.95	704.02	26.53	0.41
6	842.89	29.05	0.52	848.68	761.88	43.27	0.93
7	893.04	29.43	1.29	914.26	875.68	20.1	0.34
8	956.69	26.12	5.31	1001.06	916.19	45.94	3.29
9	1097.5	23.27	4.56	1138	1002.98	77.69	4.81
10	1153.43	25.97	0.44	1172.72	1139.93	19.08	0.13
11	1199.72	26.13	0.23	1207.44	1174.65	19.01	0.11
12	1220.94	26	4.44	1398.39	1209.37	80.61	23.02
13	1471.69	35.99	12.96	1489.05	1400.32	23.81	4.65
14	1664.57	33.97	1.96	1668.43	1573.91	30.01	2.65
15	1726.29	26.51	0.79	1730.15	1685.79	23.26	0.19
16	1789.94	30.38	0.34	1803.44	1780.3	11.93	0.07
17	2065.76	29.9	0.03	2071.55	2050.33	11.12	0.01
18	2200.78	29.09	0.01	2202.71	2073.48	68.44	0.03
19	2264.43	28.84	1.2	2314.58	2212.35	54.64	1.18
20	2389.8	28.15	1.8	2416.81	2343.51	38.83	0.88
21	2465.03	28.05	0.11	2470.81	2418.74	28.48	0.06
22	2542.18	27.31	0.42	2586.54	2472.74	63.64	0.36
23	2594.26	27.49	0.21	2785.21	2586.54	105.78	1.8
24	2810.28	32.07	0.11	2814.14	2787.14	13.23	0.02
25	2854.65	28.32	3.27	2883.58	2816.07	35.47	1.74
26	2912.51	29.17	7.84	3134.33	2885.51	74.31	4.45
27	3427.51	41.98	0.6	3431.36	3145.9	70.9	7.76
28	3489.23	39.68	0.2	3493.09	3450.65	16.56	0.03
29	3633.89	33.34	1.19	3643.53	3618.46	11.7	0.18
30	3697.54	30.31	1.26	3703.33	3682.11	10.85	0.24
31	3749.62	28.41	0.52	3753.48	3720.69	17.42	0.28
32	3759.26	28.5	0.5	3776.62	3755.4	11.3	0.07
33	3940.57	30.83	0.38	3961.79	3934.78	13.68	0.07

Date/Time; 5/13/2025 2:36:29 AM

FTIR Analysis of Diflunisal–Poloxamer 407 Mixture

The FTIR spectrum of the Diflunisal–Poloxamer 407 mixture exhibited distinct absorption bands corresponding to both the drug and the polymer, indicating their mutual compatibility. A broad band in the **3200–3600 cm⁻¹** range was attributed to **O–H stretching vibrations** from Diflunisal and the hydroxyl groups of Poloxamer 407. Strong bands between **2850–2920 cm⁻¹** were assigned to **aliphatic C–H stretching** of the polyethylene oxide and polypropylene oxide chains in the polymer. A sharp peak near **1700–1720 cm⁻¹** confirmed **C=O stretching** of Diflunisal's carboxylic acid group. Peaks within **1600–1500 cm⁻¹** indicated **aromatic C=C stretching**, verifying the intact aromatic ring of the drug.

Additional bands in the **1100–1300 cm⁻¹** region were linked to **C–O–C stretching** vibrations of ether linkages in Poloxamer 407. The retention of all characteristic peaks without notable shifts or loss suggests **no chemical interaction**, affirming the **compatibility of Diflunisal and Poloxamer 407** for formulation development.

Sophisticated Analytical Instrumental Laboratory,
School of Pharmaceutical Sciences, RGPV, Bhopal.

SHIMADZU

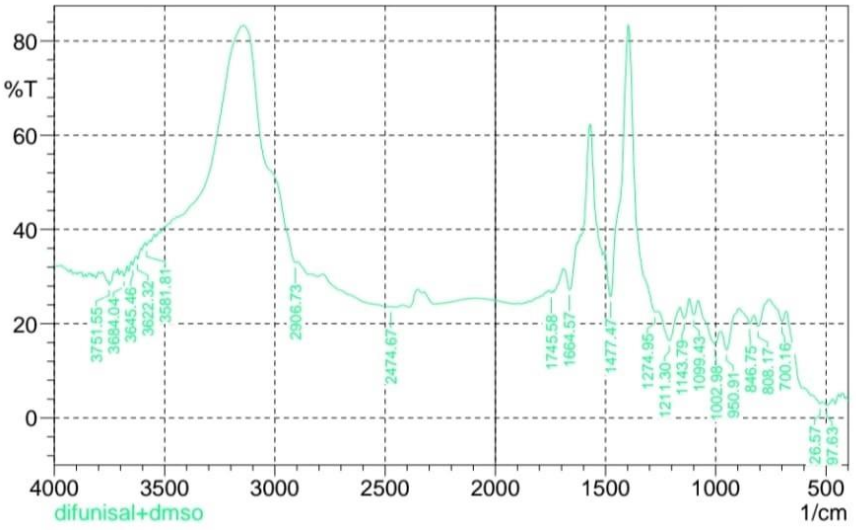

No.	Peak	Intensity	Corr. Intensity	Base (H)	Base (L)	Area	Corr. Area
1	497.63	2.619	0.305	513.07	491.85	32.568	0.368
2	526.57	3.021	0.625	561.29	518.85	60.316	1.217
3	700.16	20.433	2.846	758.02	680.87	49.534	1.538
4	808.17	19.451	3.173	825.53	758.02	44.247	1.653
5	846.75	19.928	2.271	894.97	825.53	46.241	1.226
6	950.91	14.445	5.484	977.91	894.97	60.913	4.073
7	1002.98	15.676	4.277	1080.14	977.91	74.01	5.519
8	1099.43	21.879	3.228	1120.64	1080.14	25.575	1.27
9	1143.79	21.161	3.146	1163.08	1120.64	27.42	1.405
10	1211.3	16.393	6.683	1265.3	1163.08	72.027	6.87
11	1274.95	22.473	4.621	1396.46	1265.3	59.307	11.814
12	1477.47	25.722	21.628	1504.48	1396.46	40.489	11.831
13	1664.57	27.162	6.486	1685.79	1629.85	28.81	2.748
14	1745.58	26.603	0.446	1757.15	1739.79	9.917	0.064
15	2474.67	23.585	0.094	2781.35	2470.81	183.189	5.76
16	2906.73	33.011	2.08	3142.04	2897.08	67.998	-0.496
17	3581.81	36.549	0.846	3589.53	3566.38	9.97	0.107
18	3622.32	33.7	1.084	3628.1	3606.89	9.754	0.122
19	3645.46	32.382	1.102	3651.25	3628.1	11.044	0.128
20	3684.04	30.041	1.43	3691.75	3670.54	10.834	0.229
21	3751.55	28.239	1.221	3757.33	3728.4	15.413	0.298

Comment;
difunisal+dmso

Date/Time; 5/13/2025 1:50:47 AM
No. of Scans;

FTIR Analysis of Diflunisal–DMSO Mixture

The FTIR spectrum of the Diflunisal–DMSO mixture exhibited characteristic absorption bands from both the drug and the solvent, indicating their compatibility. A broad band between **3200–3600 cm⁻¹** was attributed to **O–H stretching** of Diflunisal's carboxylic acid group. The **~2900 cm⁻¹** band corresponded to **C–H stretching vibrations**. A sharp peak in

the **1700–1720 cm⁻¹** range confirmed **C=O stretching** of the carboxylic acid moiety. Peaks between **1600–1500 cm⁻¹** were assigned to **aromatic C=C stretching**, indicating the preserved aromatic structure. Additionally, bands in the **1000–1100 cm⁻¹** region were attributed to **S=O stretching** vibrations of DMSO. The retention of all major Diflunisal peaks without significant shifts or loss confirmed the **absence of chemical interaction**, supporting the **compatibility of Diflunisal with DMSO**.

Sophisticated Analytical Instrumental Laboratory,
School of Pharmaceutical Sciences, RGPV, Bhopal.

SHIMADZU

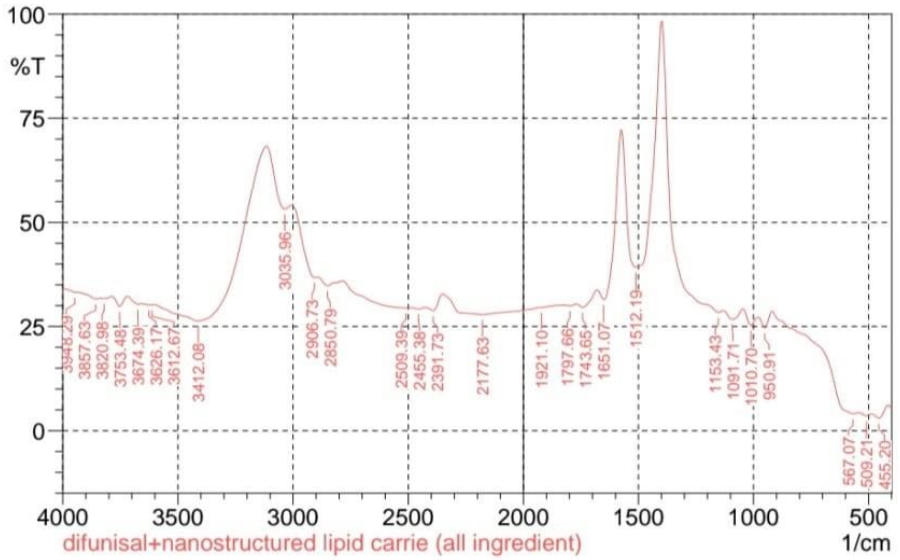

No.	Peak	Intensity	Corr. Intensity	Base (H)	Base (L)	Area	Corr. Area
1	455.2	2.99	1.95	486.06	416.62	97.48	6.99
2	509.21	3.57	0.57	542	487.99	76.33	1.73
3	567.07	4.07	1.74	918.12	543.93	312.03	5.09
4	950.91	24.69	3.21	979.84	920.05	34.66	1.55
5	1010.7	25.34	2.82	1045.42	981.77	36.49	1.5
6	1091.71	26.76	2.26	1130.29	1047.35	46.25	1.72
7	1153.43	28.37	5.97	1398.39	1132.21	115.78	42.34
8	1512.19	39.21	42.23	1573.91	1400.32	48.88	36.04
9	1651.07	31.44	12.46	1678.07	1575.84	39.49	8.48
10	1743.65	29.62	1.79	1770.65	1680	46.17	1.41
11	1797.66	29.95	0.28	1815.02	1772.58	22.12	0.1
12	1921.1	29.58	0.01	1923.03	1855.52	35.46	0.01
13	2177.63	27.86	3.64	2349.3	1923.03	230.22	14.25
14	2391.73	28.78	2.23	2424.52	2351.23	38.27	1.18
15	2455.38	29.24	0.3	2492.03	2426.45	34.87	0.14
16	2509.39	29.49	0.35	2785.21	2493.96	147.16	5.2
17	2850.79	34.81	1.69	2893.22	2787.14	47.6	1.03
18	2906.73	36.75	1.93	3005.1	2895.15	39.72	1.44
19	3035.96	53.21	4.74	3115.04	3007.02	25.65	2.28
20	3412.08	26.36	18.58	3597.24	3116.97	220.98	56.98
21	3612.67	30.19	0.05	3618.46	3599.17	10.02	0.01
22	3626.17	30.17	0.11	3639.68	3620.39	10.02	0.02
23	3674.39	30.34	0.54	3718.76	3660.89	29.43	0.25
24	3753.48	29.81	2.44	3786.27	3720.69	33.27	1.05
25	3820.98	31.71	0.2	3830.63	3788.19	21.07	0.1
26	3857.63	31.63	0.48	3894.28	3838.34	27.71	0.2
27	3948.29	33.18	0.14	4000.36	3940.57	28.3	0.02

Comment;
difunisal+nanostructured lipid carrie (all ingredient)

Date/Time; 5/13/2025 2:01:36 AM
No. of Scans;
Resolution;

FTIR Analysis of Diflunisal-Loaded Nanostructured Lipid Carrier

The FTIR spectrum of the Diflunisal-loaded NLC displayed characteristic absorption bands corresponding to both the drug and lipid excipients, confirming successful incorporation. A broad band between **3200–3600 cm^{-1}** was attributed to **O–H stretching**, indicating the presence of phenolic and carboxylic groups from Diflunisal and lipid components. Peaks around **3000–3100 cm^{-1}** and **2850–2920 cm^{-1}** were assigned to **aromatic and aliphatic C–H stretching**, respectively, reflecting contributions from both the drug and lipid matrix. A prominent band in the **1680–1710 cm^{-1}** range confirmed **C=O stretching** vibrations from Diflunisal's carboxylic acid and lipid ester groups. Peaks between **1600–1500 cm^{-1}** indicated **aromatic C=C stretching**, verifying the structural integrity of Diflunisal. Additional bands in the **1200–1300 cm^{-1}** region were linked to **C–O stretching**, while those between **1000–1300 cm^{-1}** corresponded to **C–F stretching**, confirming the presence of fluorinated aromatic rings. The retention of all major Diflunisal peaks with minor shifts and reduced intensity suggests **no significant chemical interaction**, supporting the **compatibility and successful entrapment of the drug within the NLC system**.

Photomicrograph of Difunisal loaded Nanostructured Lipid Carriers (NLCs)

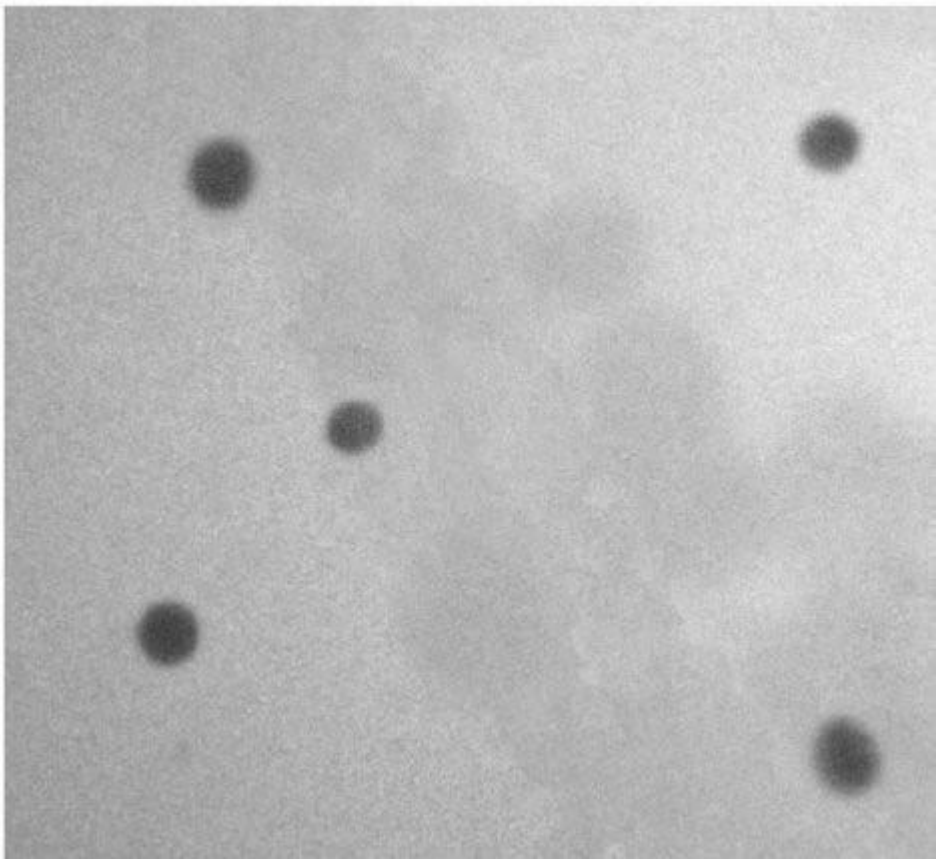

Fig. 2: Drug Loaded NLC.

Table 4: Entrapment Efficiency and Drug Loss.

S NO.	Formulation Code	Entrapment Efficiency	Drug Loss
1.	F1	99.04	0.9517
2.	F2	99.11	0.8819
3.	F3	99.30	0.6903
4.	F4	99.04	0.9507
5.	F5	99.31	0.6872

Entrapment Efficiency and Drug Loss Evaluation

The entrapment efficiency and drug loss of nanostructured lipid carrier (NLC) formulations F1–F5 were assessed to evaluate drug incorporation within the lipid matrix. Entrapment efficiency reflects the system's ability to encapsulate the drug, while drug loss indicates leakage during formulation.

All formulations demonstrated **high entrapment efficiency (>99%)**, confirming the effectiveness of the selected lipids and preparation method. Formulation **F1** showed an efficiency of **99.048%** with a drug loss of **0.9517%**, while **F2** improved slightly with **99.118%** efficiency and **0.8819%** drug loss.

F3 exhibited **99.309%** entrapment and the **lowest drug loss (0.6903%)**, suggesting optimal drug–lipid interaction and enhanced formulation stability. In contrast, **F4** had **99.049%** efficiency with a higher drug loss of **0.9507%**, possibly due to lipid matrix saturation.

F5 achieved the **highest entrapment efficiency (99.3128%)**, though its drug loss (**0.6872%**) was marginally higher than F3. This indicates that increased component concentration may enhance drug loading but could slightly elevate drug leakage.

Overall, an **inverse relationship** was observed between entrapment efficiency and drug loss. **F5** was identified as the most efficient in drug encapsulation, while **F3** exhibited the best drug retention, making both suitable for further development.

Viscocity of Nanostructured Lipid Carriers (NLCs)

Viscosity Evaluation of Diflunisal-Loaded NLC Dispersion

The viscosity of the Diflunisal-loaded nanostructured lipid carrier (NLC) dispersion was assessed using a Brookfield digital viscometer to evaluate its rheological behavior, flow characteristics, and formulation stability. Measurements were conducted at room temperature using a suitable spindle (e.g., spindle no. 64) at varying rotational speeds (e.g., 20 rpm). The

optimized formulation exhibited a viscosity of approximately 2790 cP, indicating favorable flow properties and physical stability. The resistance encountered by the rotating spindle was recorded, and viscosity values were expressed in **centipoise (cP)**. These findings confirm the dispersion's suitability for pharmaceutical processing and potential application in drug delivery systems.

Viscosity Evaluation of Optimized NLC-Based Gel

The viscosity of the optimized nanostructured lipid carrier (NLC)-based gel was measured at room temperature using a Brookfield digital viscometer. The assessment was conducted at a rotational speed of **12 rpm** with an appropriate spindle. The gel exhibited a viscosity of approximately **17,310 cP**, indicating a suitable consistency for topical application. This viscosity supports **ease of spreading, user comfort, and formulation stability**. The single-speed measurement provided consistent and reproducible data, confirming the gel's physical robustness and suitability for pharmaceutical use.

Table 5: pH measurement of Difunisal loaded Nanostructured Lipid Carriers (NLCs) Dispersion.

S.no	Formulations	pH
1.	F1	7.15
2.	F2	7.26
3.	F3	6.94
4.	F4	7.25
5.	F5	7.02

pH Evaluation of Optimized NLC-Based Gel

The pH of the optimized NLC-based gel was assessed to confirm its compatibility with skin physiology and its appropriateness for topical application. The formulation exhibited a pH of approximately 5.9, which falls within the acceptable dermal range of 4.5–6.5.

This slightly acidic pH aligns closely with the natural pH of human skin, suggesting minimal risk of irritation and supporting the formulation's dermatological safety. The result indicates that the gel is well-suited for topical drug delivery, potentially enhancing patient compliance by preserving skin integrity.

Spreadability Evaluation of Optimized NLC-Based Gel

The spreadability of the optimized nanostructured lipid carrier (NLC)-based gel was assessed to determine its ease of application and uniform distribution over the skin. Adequate

spreadability is essential for topical formulations to ensure effective coverage and enhance patient compliance. The optimized gel exhibited a **satisfactory spreadability value**, reflecting its ideal consistency and favorable application properties for dermal use.

The spreadability of the gel was calculated using the following formula:

$$S = M \times L / T$$

Where,

S = Spreadability (g·cm/s)

M = Weight tied to the upper slide (2000 g)

L = Length of the glass slide moved (5 cm)

T = Time taken to separate the slides (1800s)

Spreadability of Optimized NLC-Based Gel

The optimized nanostructured lipid carrier (NLC)-based gel exhibited a spreadability value of **5.56 g·cm/s**, indicating **adequate consistency and smooth application**. This result confirms the gel's favorable spreading behavior, ensuring **uniform distribution on the skin** and supporting its suitability for **topical administration**.

pH Evaluation of Optimized NLC-Based Gel

The pH of the optimized nanostructured lipid carrier (NLC)-based gel was measured to assess its **suitability for topical application** and **skin compatibility**. The gel exhibited a pH of approximately **5.9**, which falls within the acceptable range of **4.5–6.5** for dermal formulations. This slightly acidic pH aligns with the natural skin environment, supporting **skin integrity** and **minimizing irritation**. The result confirms that the formulation is **safe, non-irritating**, and appropriate for **topical drug delivery**.

Table 6: for Stability Study of Result of Difunisal loaded Nanostructured Lipid Carriers (NLCs) gel.

Storage Condition	Appearance	pH	Viscocity	Spreadability
Room Temperature (25°C ± 2°C)	No phase separation, no discolouration, smooth texture	5.8	Slight increased	5.0
Refrigeration Temperature (4°C ± 2°C)	No phase separation, no discolouration, smooth texture	5.5	Increased viscosity	4.8
Accelerated Conditions (40°C ± 2°C)	Slight phase separation, slight discolouration.	5.5	Increased viscosity	4.8

Stability Studies of Diflunisal-Loaded NLC Gel

Room Temperature (25 ± 2°C)

After one month of storage, the gel showed **no visible signs of phase separation, discoloration, or texture change**. A slight increase in viscosity was noted, while the pH remained stable at **5.8** (initial: 5.9). **Spreadability remained at 5 cm**, indicating consistent application properties. These findings confirm **good physical stability** at room temperature.

Refrigerated Conditions (4 ± 2°C)

The gel retained a **smooth, uniform texture** with **no phase separation or discoloration**. Viscosity increased slightly, but **pH remained constant at 5.9**, and **spreadability was unchanged at 5 cm**, indicating **excellent stability** under cold storage.

Accelerated Conditions (40 ± 2°C)

Storage at elevated temperature led to a **slight viscosity increase**, **mild phase separation**, a **pH drop to 5.5**, and a **reduction in spreadability to 4.8 cm**. These changes suggest **incipient instability** under stress conditions.

The diflunisal-loaded NLC gel demonstrated **robust stability** at both room and refrigerated temperatures over one month. However, **accelerated conditions induced minor instability**, indicating that **storage at elevated temperatures should be avoided** to preserve formulation integrity.

Table 7: Cumulative Percentage Drug Release of Formulations.

Time(hr)	F1	F2	F3	F4	F5
1	26.18	28.45	30.41	24.43	22.43
2	36.67	38.32	41.38	34.08	32.96
3	46.88	48.95	52.96	44.54	42.64
4	56.77	58.59	63.69	54.26	52.84
5	66.56	68.43	72.08	64.53	61.21
6	73.09	75.09	79.54	71.28	68.93
7	80.65	82.65	86.97	78.52	75.52
8	85.67	88.43	91.64	83.97	80

Drug Release Study

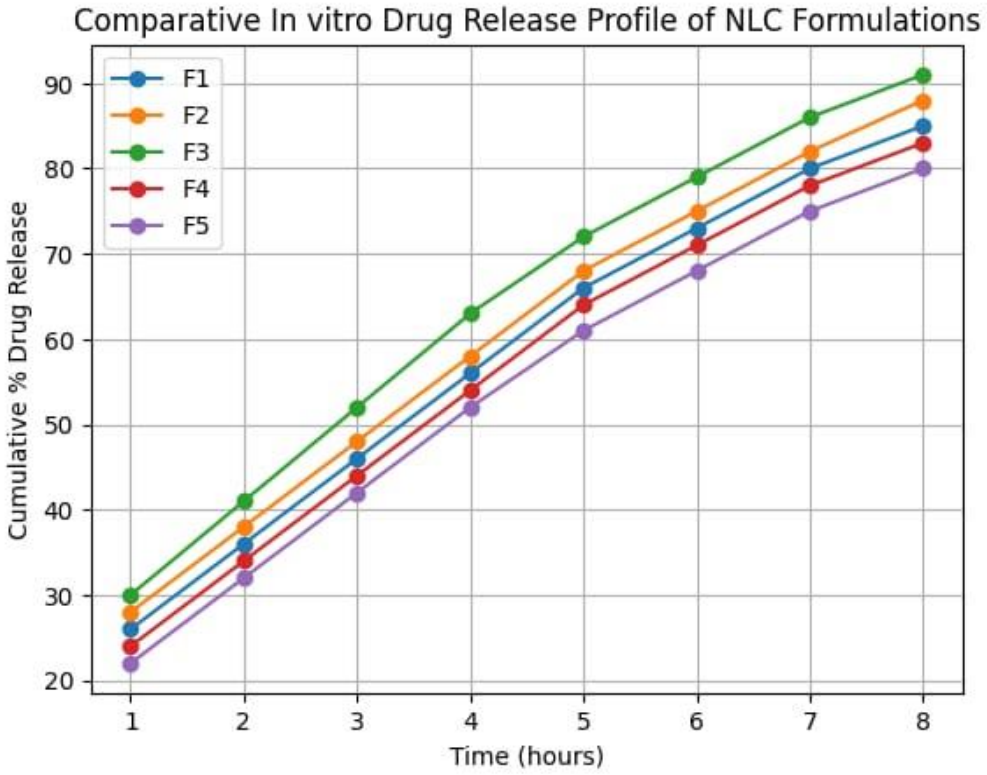

Fig -3: Graph for drug release

The cumulative drug release profiles of NLC formulations F1–F5, as illustrated in Table 7and Figure 3, demonstrated a steady increase in release over an 8-hour period. At the 1-hour mark, drug release ranged between 22% and 30%, gradually rising to 80–91% by the end of the study.

The lack of an initial burst effect suggests effective drug entrapment within the lipid matrix. This consistent, controlled release behavior underscores the potential of NLCs for sustained drug delivery. Notably, formulation F3 exhibited the highest cumulative release, whereas F5 showed the slowest and most controlled release pattern.

Such sustained release characteristics are particularly beneficial for topical applications, as they may support prolonged therapeutic levels at the application site and reduce dosing frequency.

In-vitro Drug Release of the optimized NLC gel formulation

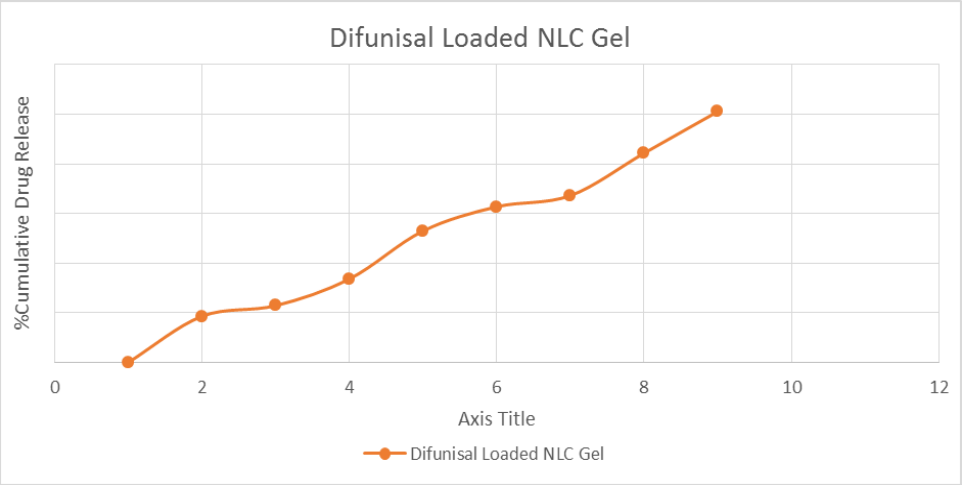

Figure 4.

In-vitro drug release profile of optimized NLC gel through egg membrane using PBS pH 7.4

The in-vitro drug release profile of the optimized NLC gel formulation, evaluated using the egg membrane diffusion method, showed a gradual and sustained release of the drug over a period of 10 hours. The cumulative percentage drug release increased progressively with time, indicating controlled drug diffusion through the egg membrane. The sustained release behavior may be attributed to the lipid matrix of the NLC system and the gel network, which together retard drug diffusion. The observed release pattern suggests the suitability of the developed NLC gel for topical drug delivery.

Particle size and size distribution

Dynamic light scattering analysis revealed that NLC Gel 1 exhibited a z-average particle size of 213.0 nm with a polydispersity index (PDI) of 0.550, indicating a moderately polydisperse system. The intensity-weighted size distribution showed a dominant peak at 185.6 nm contributing 76.7% intensity, confirming the formation of nanosized lipid carriers. Minor secondary peaks were observed at 1682 nm (9.9%) and 4372 nm (13.4%), which may be attributed to particle aggregation or gel-associated larger structures. Overall, the DLS results confirm successful formation of NLCs within the nanometric range, suitable for topical drug delivery applications.

Results

		Size (d.nm):	% Intensity:	St Dev (d.n...
Z-Average (d.nm): 213.0	Peak 1:	185.6	76.7	84.20
PdI: 0.550	Peak 2:	4372	13.4	964.4
Intercept: 0.925	Peak 3:	1682	9.9	546.7
Result quality : Good				

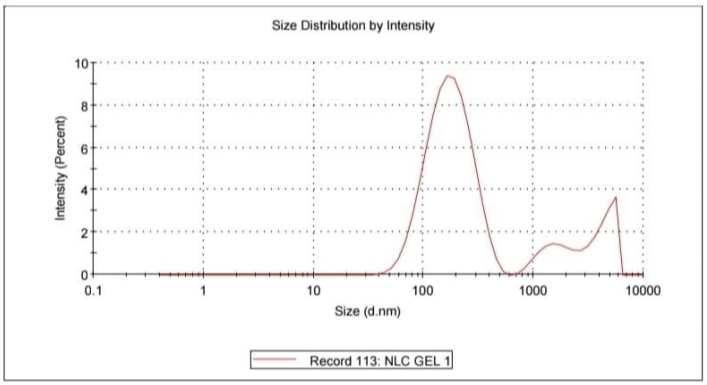

Zeta potential

The zeta potential of NLC Gel 1 was found to be −10.3 ± 4.9 mV, indicating a moderately charged surface. Although the absolute zeta potential value is lower than ±30 mV, the formulation stability can be attributed to steric stabilization provided by lipid components and surfactants, which is common in lipid-based nanocarrier systems. The observed zeta potential is considered sufficient for maintaining short-term physical stability of the NLC gel formulation.

Results

		Mean (mV)	Area (%)	St Dev (mV)
Zeta Potential (mV): -10.3	Peak 1:	-10.3	100.0	4.90
Zeta Deviation (mV): 4.90	Peak 2:	0.00	0.0	0.00
Conductivity (mS/cm): 0.338	Peak 3:	0.00	0.0	0.00
Result quality : See result quality report				

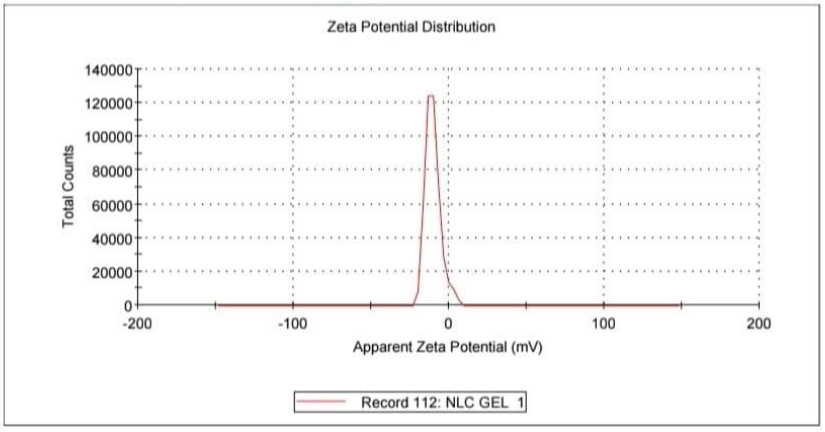

DISCUSSION

Diflunisal-loaded nanostructured lipid carrier (NLC)-based gels were successfully formulated and evaluated for enhanced topical drug delivery. All five formulations (F1–F5) were assessed for key parameters including entrapment efficiency, drug loss, pH, viscosity, FTIR compatibility, and in vitro drug release.

The entrapment efficiency of all formulations was remarkably high, ranging from 99.04% to 99.31%, indicating excellent drug incorporation within the lipid matrix. Among them, formulation F5 exhibited the highest entrapment efficiency (99.31%) with the lowest drug loss (0.6872%), followed closely by F3 (99.30%, 0.6903%). These results confirm the stability of the drug within the lipid core and minimal leakage during formulation.

The pH of the optimized NLC-based gel was found to be approximately 5.9, which lies within the acceptable dermal range (4.5–6.5), ensuring skin compatibility and minimizing the risk of irritation. This slightly acidic pH also aligns with the natural pH of human skin, supporting its suitability for topical application.

FTIR spectral analysis confirmed the absence of significant chemical interactions between diflunisal and the excipients, as evidenced by the retention of characteristic peaks in the optimized formulation. This indicates the chemical stability of the drug within the NLC system.

Viscosity measurements revealed that the gel possessed suitable rheological properties for topical application, offering ease of spreadability and adequate retention at the site of application. The formulation exhibited pseudoplastic flow behavior, which is desirable for patient comfort and controlled application.

In vitro drug release studies demonstrated a sustained and controlled release pattern over 8 hours, with cumulative drug release ranging from 80% to 91%. Formulation F3 showed the highest cumulative release, while F5 exhibited a slower and more controlled release profile.

Overall, the optimized NLC-based gel formulation (F5) demonstrated a favorable balance of high entrapment efficiency, minimal drug loss, sustained release, and excellentphysicochemical stability, making it a promising candidate for effective topical delivery of diflunisal.

CONCLUSION

The study successfully developed and characterized diflunisal-loaded nanostructured lipid carrier (NLC)-based gel formulations for topical drug delivery. All formulations exhibited high entrapment efficiency (>99%) and minimal drug loss, with formulation F5 showing the most favorable profile (99.31% EE, 0.6872% drug loss).

The optimized gel demonstrated a skin-compatible pH (~5.9), suitable viscosity, and no significant drug–excipient interactions, as confirmed by FTIR analysis. In vitro release studies revealed a sustained and controlled drug release over 8 hours, with F3 showing the highest release and F5 offering the most prolonged release behavior.

These findings suggest that the developed NLC-based gel system, particularly formulation F5, holds significant potential for enhancing the topical delivery of diflunisal, offering improved therapeutic efficacy, reduced dosing frequency, and better patient compliance.

Ethical Approval: there is no requirement for ethical Approval in this research.

Conflict of Interest

The author declares no conflict of interest. This research was conducted independently and was entirely self-funded.

REFERENCES

1. Shivani Rathor, Dr. Tanu Bhargava, Dr. Praveen Khirwadkar, Dr. Kamlesh Dashora, Nanostructured Lipid Carriers: A Versatile Platform for Drug Delivery Across Therapeutic areas, Int. J. of Pharm. Sci., 2025; 3(12): 2733-2757. https://doi.org/10.5281/zenodo.17966504
2. Kreutz, W. Diflunisal for the Treatment of Cancer. U.S. Patent, December 2006; 20060293390: 28.
3. Entellas, C.M.; Insa, B.R.; Reig, B.N.; Gavalda, B.N. Therapy for Transthyretin-Associated Amyloidosis. U.S. Patent 2020390733A1, 17 December 2020.
4. Tojo, K.; Sekijima, Y.; Kelly, J.W.; Ikeda, S. Diflunisal stabilizes familial amyloid polyneuropathy-associated transthyretin variant tetramers in serum against dissociation required for amyloidogenesis. Neurosci. Res., 2006; 56: 441–449.

5. Berk, J.L.; Suhr, O.B.; Sekijima, Y.; Yamashita, T.; Heneghan, M.; Zeldenrust, S.R.; Ando, Y.; Ikeda, S.; Gorevic, P.; Merlini, G.; et al. The Diflunisal Trial: Study accrual and drug tolerance. Amyloid, 2012; 19(1): 37–38.
6. Berk, J.L.; Suhr, O.B.; Obici, L.; Sekijima, Y.; Zeldenrust, S.R.; Yamashita, T.; Heneghan, M.A.; Gorevic, P.D.; Litchy, W.J.; Wiesman, J.F.; et al. Diflunisal Trial, Consortium. Repurposing diflunisal for familial amyloid polyneuropathy: A randomized clinical trial. JAMA, 2013; 310: 2658–2667.
7. Sekijima, Y.; Tojo, K.; Morita, H.; Koyama, J.; Ikeda, S. Safety and efficacy of long-term diflunisal administration in hereditary transthyretin (ATTR) amyloidosis. Amyloid, 2015; 22: 79–83.
8. Ikram, A.; Donnelly, J.P.; Sperry, B.W.; Samaras, C.; Valent, J.; Hanna, M. Diflunisal tolerability in transthyretin cardiac amyloidosis: A single center's experience. Amyloid, 2018; 25: 197–202.
9. Castaño, A.; Helmke, S.; Alvarez, J.; Delisle, S.; Mathew, S.; Maurer, M.S. Diflunisal for ATTR Cardiac Amyloidosis. Congest. Heart Fail., 2012; 18: 315–319.
10. Rosenblum, H.; Castano, A.; Alvarez, J.; Goldsmith, J.; Helmke, S.; Maurer, M.S. TTR (transthyretin) stabilizers are associated with improved survival in patients with TTR cardiac amyloidosis. Circ. Heart Fail., 2018; 11: e004769.
11. Yadav, J.D.; Othee, H.; Chan, K.A.; Man, D.C.; Belliveau, P.P.; Towle, J. Transthyretin Amyloid Cardiomyopathy-Current and Future Therapies. Ann. Pharmacother, 2021.
12. Kearney, P.M.; Baigent, C.; Godwin, J.; Halls, H.; Emberson, J.R.; Patrono, C. Do selective cyclo-oxygenase-2 inhibitors and traditional non-steroidal anti-inflammatory drugs increase the risk of atherothrombosis? Meta-analysis of randomised trials. BMJ, 2006; 332: 1302–1308.
13. Wallace, J.L. Pathogenesis of NSAID-induced gastroduodenal mucosal injury. Best Pract. Res. Clin. Gastroenterol, 2001; 15: 691–703.
14. Mukherjee, D.; Nissen, S.E.; Topol, E.J. Risk of cardiovascular events associated with selective COX-2 inhibitors. JAMA, 2001; 286: 954–959. 2, 3S–8S**.**
15. Bashir M, Ahmad J, Asif M. Nanoemulgel, an Innovative Carrier for Diflunisal Topical Delivery with Profound Anti-Inflammatory Effect: in vitro and in vivo Evaluation International Journal of Nanomedicine, 2021; 16.
16. Sathish babu*K, Karun Babu K., Vijayaraj S. SPECTROPHOTOMETRIC DETERMINATION OF DIFLUNISAL FROM ITS FOMULATION BY HYDROTOPHY TECHNIQUE IJMCA, 2012; 2(2): 101-1058.

17. Sahoo L. Design development and evaluation of transdermal patch loaded with nanostructured lipid carrier containing selected drugs for bioavailability enhancement [thesis]. Centurion University of Technology and Management; 2024. Available from: http://hdl.handle.net/10603/600651
18. Czajkowska-Ko´snik, A.; Szyma´nska, E.; Winnicka, K. Nanostructured Lipid Carriers (NLC)-Based Gel Formulations as Etodolac Delivery: From Gel Preparation to Permeation Study. Molecules, 2023; 28: 235. https:// doi.org/10.3390/molecules28010235
19. Cirri M, Maestrini L, Maestrelli F. Design, characterization and in vivo evaluation of nanostructured lipid carriers (NLC) as a new drug delivery system for hydrochlorothiazide oral administration in pediatric therapy DRUG DELIVERY, 2018; 25(1): 1910–1921. https://doi.org/10.1080/10717544.2018.1529209.
20. Sethuraman N, Shanmuganathan S, Sandhya K, Design, Development and Characterization of Nano Structured Lipid Carrier for Topical Delivery of Aceclofenac Indian Journal of Pharmaceutical Education and Research, Oct-Dec, 201; 52(4).
21. Kaur LP, Garg R, Gupta GD. Development and evaluation of topical gel of minoxidil from different polymer bases in application of alopecia. Int. J. Pharmacy and Pharm. Sci., 2010; 2: 43-7.
22. Nosratabadi M, Rahimnia S, Barogh R. Luliconazole-loaded nanostructured lipid carrier: formulation, characterization, and in vitro antifungal evaluation against a panel of resistant fungal strains. Scientific Reports, 2024; 14: 30708. | https://doi.org/10.1038/s41598-024-79225-1.